Lead Substitution in Synaptotagmin: A Case Study

M.-C. van Severen, J.-P. Piquemal, and O. Parisel*

UMR 7616, Laboratoire de Chimie Théorique, UPMC Université Paris 06, case courrier 137, 4 place Jussieu F-75005, Paris, France, and UMR 7616, Laboratoire de Chimie Théorique, CNRS, case courrier 137, 4 place Jussieu F-75005, Paris, France

Received: October 23, 2009; Revised Manuscript Received: February 8, 2010

Quantum chemistry computations have been used to investigate the possibility of a Pb^{2+}/Ca^{2+} substitution in the three calcium sites of the synaptotagmin enzyme. Provided explicit cation solvation is taken into account, it is shown that the substitution is energetically feasible and induces a strong reorganization of the Ca^{2+}-coordinating sites, which may preclude the enzyme for any efficient role when lead poisoning occurs.

I. Introduction and Structural Modeling

Synaptotagmin is an antigen calcium protein first described by Matthew,[1] and identified by Perin.[2,3] It expresses at the outer part of synaptic vesicles and plays an essential role in supporting neurotransmitters as communication signals relying on tuned Ca^{2+} fluxes.

It is now well established that saturnism (lead poisoning) can induce neurological dysfunctions, the intimate molecular origins of which still have not been fully characterized. As Godwin[4] and Suszkiw[5] have recently shown that synaptotagmin can be perturbed by lead, thus providing another example of a metalloprotein targeted by Pb^{2+}, we have found of interest to perform some molecular modeling of this system. For that purpose we here follow and refine a procedure initially established to investigate commonly used lead chelators interacting with metallic oligoelements, or lead substitution in both the calmodulin and the ALAD (δ-aminolevulinic acid dehydratase) enzymes.[6,7]

A simple view of synaptotagmin is provided in Figure 1: it reveals that the three calcium sites are located on the surface of the protein between two external loops that connect three β-sheets: this suggests that cation/cation exchanges with the outer medium can be envisioned. These three calcium sites have been modeled according to the description given in Figure 1: only their first coordination spheres have been retained, which led to the consideration of about 85 atoms per site. On the basis of the 1UOV X-ray structure of synaptotagmin,[8] these models will thereafter be referred to as 1UOV_M_n where M stands for the dication involved (Ca in the native form, or Pb after substitution), and index n allows differentiating the three sites. From the 1UOV crystallographic data, the calcium−calcium distances amount to: $(Ca_1,Ca_2) = 3.71$ Å, $(Ca_2,Ca_3) = 4.43$ Å, and $(Ca_1,Ca_3) = 7.41$ Å. Each site can be described using its native Ca coordination before substitution by Pb^{2+} and using the 1UOV_Ca_n nomenclature:

- 1UOV_Ca_1: three water molecules (O1, O2, and O3), two η^1-coordinated formate anions (O5 and O6), one η^2-coordinated formate anion (O7 and O8), and the carbonyl group of an amide function (O4)
- 1UOV_Ca_2: one water molecule (O8), two η^1-coordinated formate anions (O4 and O1), two η^2-coordinated formate anions (O2, O3, O5, and O6), and the carbonyl group of an amide function (O7)
- 1UOV_Ca_3: four water molecules (O2, O5, O6, and O7), one η^2-coordinated formate anion (O3 and O4), and the carbonyl group of an amide function (O1).

When referring to a substitution, we will shortly use the notation 1UOV_Ca_n/Pb_n.

II. Computational Protocol

II.1. Methodology. The calculations have been performed using the GAUSSIAN03 package[9] within the B3LYP formalism. This functional[10,11] was chosen as it has proven to provide geometries and energies close to the CCSD(T) approach.[12−16] The standard 6-31+G** basis set was used to describe the H, C, N, and O atoms. Scalar relativistic pseudopotentials[17] were used for Pb^{2+}: for the final results reported, the large-core relativistic SDD pseudopotentials by Dolg et al.[18] (78 electrons *pseudized* for neutral Pb) coupled to a (4s4p1d)/[2s2p1d] contraction to describe the valence electrons. These functional, basis set, and pseudopotential have been successfully employed in our previous works devoted to Pb^{2+} or to other heavy cations and have proven to reproduce 4-component relativistic computations.[19−21]

Several levels of geometry optimization have been considered. First, starting from the atomic PDB coordinates, only hydrogen atoms have been optimized (thereafter, H_{opt}). Second, the metallic cation also is optimized (M_{opt}). Then all atoms are relaxed, except those directly linked to the proteic skeleton (L_{opt}). Finally, all atomic positions are optimized (T_{opt}) and the nature of the stationary points encountered has been characterized by a vibrational analysis performed within the harmonic approximation, which allowed us to estimate free enthalpy ΔG values at $T = 298$ K.

II.2. Interpretative Tools: The Topological Analysis of the ELF Function. ELF (electron localization function) calculations and the topological analysis of the ELF function have been performed using the TopMod package.[22−27] We here just recall that within the framework of the topological analysis of the ELF function, space is partitioned into *basins*, each of them having a chemical meaning. Such basins are classified as[23]

(i) core basins surrounding nuclei,

(ii) valence basins characterized by their synaptic order.

Further details can be found in the above-mentioned references and in a recent review dedicated to the applications of the ELF topological analysis to biological systems.[28]

* Corresponding author. E-mail: olivier.parisel@upmc.fr.

10.1021/jp910131r
Published on Web 03/01/2010

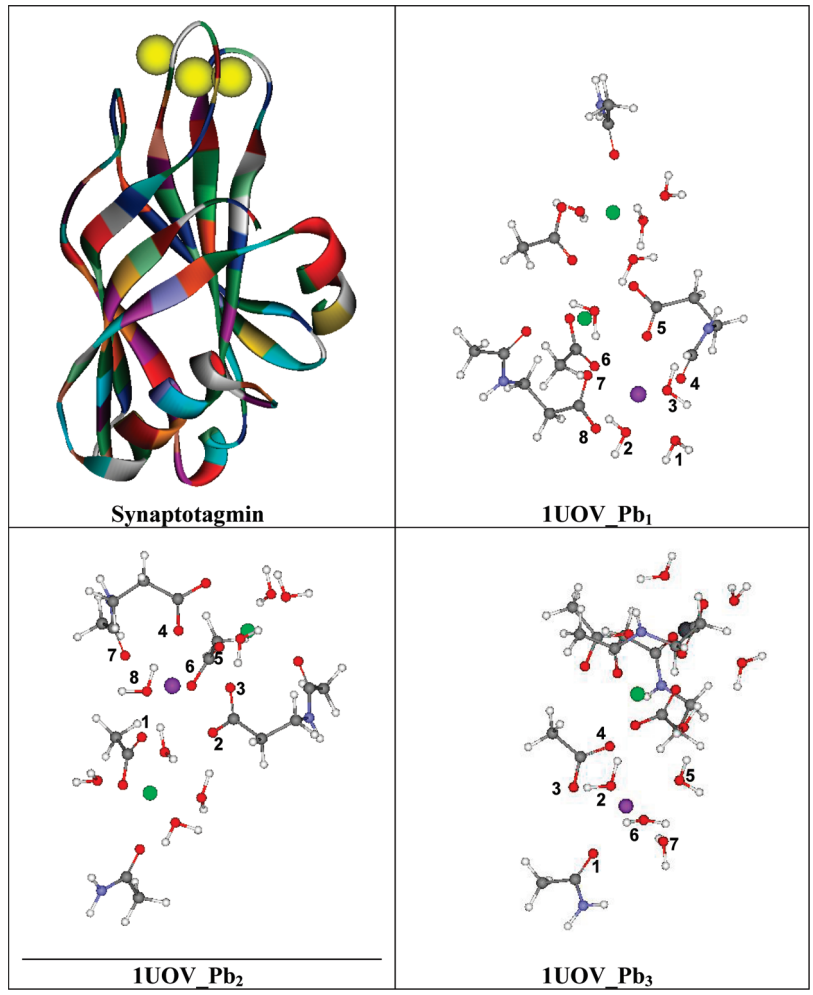

Figure 1. View of synaptotagmin showing the three calcium cations (top left; from the X-ray structure reported in ref 8), and the three models retained after Pb^{2+} substitution (before any structural relaxation), namely 1UOV_Pb_1, 1UOV_Pb_2, and 1UOV_Pb_3. Color convention: red for oxygen, green for calcium, purple for lead, gray for carbon, blue for nitrogen, and white for hydrogen.

TABLE 1: Metal−Oxygen Bond Lenghts (Å) for 1UOV_Ca_n/Pb_n at Two Levels of Geometry Optimization (See Text for Details)[a]

	M_{opt}			T_{opt}		
	1UOV_Ca_1/Pb_1	1UOV_Ca_2/Pb_2	1UOV_Ca_3/Pb_3	1UOV_Ca_1/Pb_1	1UOV_Ca_2/Pb_2	1UOV_Ca_3/Pb_3
M_n−O1	2.4/2.4	2.4/2.3	2.4/2.4	2.3/4.2	2.3/2.5	2.3/2.5
M_n−O2	2.4/2.4	2.3/2.3	2.3/2.3	2.3/3.2	2.4/2.7	2.3/2.8
M_n−O3	2.5/2.4	2.4/2.5	2.2/2.2	2.5/2.7	2.5/2.8	2.3/2.4
M_n−O4	2.5/2.5	2.4/2.4	2.3/2.4	2.3/2.7	2.3/3.0	2.6/2.8
M_n−O5	2.3/2.3	2.5/2.6	2.3/2.3	2.3/2.5	2.7/2.9	2.3/2.7
M_n−O6	2.3/2.3	2.3/2.3	2.2/2.2	2.3/2.5	2.5/2.3	2.2/2.7
M_n−O7	2.5/2.6	2.3/2.3	2.5/2.4	2.7/2.6	2.3/2.6	2.3/3.8
M_n−O8	2.4/2.4	2.5/2.5		2.5/2.7	2.4/3.4	

[a] The most important bond length increases upon substitution are underlined.

It has been shown possible to extend the ELF approach to pseudopotential approaches.[16,29] Small-core pseudopotentials provide *semiexternal cores* and allow determining the synapticity of well-defined valence basins; large-core pseudopotentials preserve the number and the properties of valence basins.[20,30]

In the present contribution, we will focus on V(Pb), the valence monosynaptic basin associated with the valence electrons of Pb^{2+}, which is chemically relevant to the electrons populating the 6s and 6p orbitals. For a given site, we will use the following notations: V(Pb) is the ELF basin defined previously, N(Pb) and ω(Pb) are respectively the population and the volume associated with this basin. ρ(Pb) is the corresponding mean charge density and is determined according to $\rho(Pb) = N(Pb)/\omega(Pb)$.[6,7,20,21]

III. Results and Discussion

III.1. Structural Studies. Table 1 collects some characteristic metal (Ca^{2+} or Pb^{2+})−ligand bond lengths for the three model active sites, using the atomic numbering depicted in Figure 1.

Starting from the X-ray coordinates, no drastic changes are observed for 1UOV_Ca_1, 1UOV_Ca_2, and 1UOV_Ca_3 when going from the H_{opt} level of optimization to the T_{opt} level, which seems to indicate that the models considered are realistic from a structural viewpoint. Things are, however, different when the substitution of Ca^{2+} by Pb^{2+} is considered. At the M_{opt} level, no strong distortions are observed between 1UOV_Ca_n and 1UOV_Pb_n, which seems to indicate that Pb^{2+} can effectively replace Ca^{2+} in the three model active sites.

TABLE 2: Population N(Pb) (Number of Electrons), Volume ω(Pb) (au^3), and Mean Electronic Density ρ(Pb) (10^{-3} e$^-$/au^3) of the V(Pb) Basin

	N(Pb)	ω(Pb)	ρ(Pb)
1UOV_Pb$_1$ (H_{opt})	2.4	114	21
1UOV_Pb$_2$ (H_{opt})	2.4	117	21
1UOV_Pb$_3$ (H_{opt})	2.4	113	21
1UOV_Pb$_1$ (T_{opt})	2.4	155	15
1UOV_Pb$_2$ (T_{opt})	2.4	146	16
1UOV_Pb$_3$ (T_{opt})	2.4	172	14

When all atoms (T_{opt}) relax, some strong deformations are observed, however. In the 1UOV_M$_1$ models, both O1 and O2 are repelled upon the Ca^{2+}/Pb^{2+} substitution: the two corresponding water molecules have been pushed out of the first coordination sphere. The same trends are observed for 1UOV_M$_2$ (O4 and O8 are strongly repelled), and for 1UOV_M$_3$ (O7 is repelled). In any case, there is also a quasi-systematic increase of the cation/other oxygen bond lengths of 0.1−0.4 Å when the T_{opt} values for 1UOV_Ca$_n$ and 1UOV_Pb$_n$ are compared. It is expected that such distortions allow the valence pair of Pb^{2+} to expand, as will be seen by means of the topological analysis of the ELF function.

III.2. ELF Analysis. Our previous studies have established that both ω(Pb) and ρ(Pb), namely the volume and the mean charge density of the ELFic V(Pb) basin, reach plateaus for high coordination numbers: ω(Pb) cannot decrease below about 150 au^3, and ρ(Pb) cannot exceed about 16.10^{-3} e$^-$/au^3.[6,7,20,21]

Table 2 reveals that the three model sites of synaptotagmin follow these rules. If 1UOV_Pb$_n$ H_{opt}-structures are considered, namely those in which we have replaced Ca^{2+} by Pb^{2+} with no optimization (except for the hydrogen atoms), values of about 115 au^3 are observed, and ρ(Pb) amounts to 21×10^{-3} e$^-$/au^3. These values show that the V(Pb) basin is too sterically constrained and that a reorganization must occur. Upon full relaxation (T_{opt}), the volume of the V(Pb) basins increases to reach values above the threshold of 150 au^3; concomitantly, ρ(Pb) decreases from 21 to about 15.10^{-3} e$^-$/au^3. These changes are driven by the expansion of V(Pb), which, consequently, induces reorganization of the ligands as described above. The emergence of V(Pb) is clearly illustrated by the ELF basins presented in Figure 2 for site 1UOV_Pb$_1$. Analogous trends are of course observed for the two other sites.

On the basis of their structural properties, lead complexes have been historically classified into two families, namely holodirected and hemidirected structures.[31] Even if a third structural class, the so-called bisdirected structure, has been predicted very recently,[32] we here seem to face such an holo-

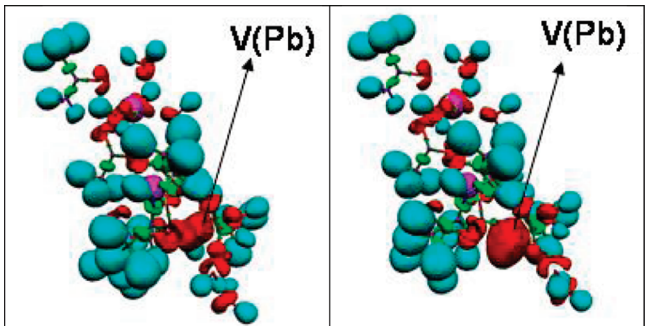

Figure 2. ELF topological analysis before (H_{opt}) and after (T_{opt}) geometry optimization.

TABLE 3: Substitution ΔE and ΔG Values (kcal/mol) for Naked Cations

	ΔE
H_{opt} (1UOV_Ca$_1$/Pb$_1$)	178
M_{opt} (1UOV_ Ca$_1$/Pb$_1$)	71
L_{opt} (1UOV_ Ca$_1$/Pb$_1$)	34
T_{opt} (1UOV_ Ca$_1$/Pb$_1$)	34
H_{opt} (1UOV_ Ca$_2$/Pb$_2$)	170
M_{opt} (1UOV_ Ca$_2$/Pb$_2$)	64
L_{opt} (1UOV_ Ca$_2$/Pb$_2$)	33
T_{opt} (1UOV_ Ca$_2$/Pb$_2$)	27
H_{opt} (1UOV_ Ca$_3$/Pb$_3$)	188
M_{opt} (1UOV_ Ca$_3$/Pb$_3$)	81
L_{opt} (1UOV_ Ca$_3$/Pb$_3$)	34
T_{opt} (1UOV_ Ca$_3$/Pb$_3$)	30
	ΔG
T_{opt} (1UOV_ Ca$_1$/Pb$_1$)	30
T_{opt} (1UOV_ Ca$_2$/Pb$_2$)	22
T_{opt} (1UOV_ Ca$_3$/Pb$_3$)	25

vs hemidirectionality competition, such as that encountered previously when either some commonly used chelators,[6] the calmodulin enzyme,[7] or model systems were investigated.[20,21] Indeed, the Ca^{2+} enzyme site usually exhibits a holodirected character, but upon substitution by Pb^{2+}, it tends to hemidirectionality by means of the expulsion of some ligands and the reduction of the coordination number in the first coordination sphere to allow the Pb^{2+} valence electrons to expand in space. This phenomenon is here clearly observed and can be quantified by both the volume and the electronic density of the V(Pb) basin.

III.3. Energetical Study. The energetic analysis related to the substitution is a difficult task as the exact nature of incoming Pb^{2+} and expelled Ca^{2+} are not known in biological conditions. We will thus consider several possibilities: the first of which, but the less probable, involves naked ions. The other ones involve hydrated cations. Of course, only T_{opt} structures will be considered to estimate ΔG values.

III.3.a. Naked Cations. In that case, the substitution equation simply reads:

$$Pb^{2+} + [1UOV\_Ca_n] \rightarrow [1UOV\_Pb_n] + Ca^{2+}$$

The corresponding ΔE and ΔG values are gathered in Table 3 for the three sites. It can be seen that all ΔE values are positive, making the substitution unfavorable. Increasing the level of optimization decreases these positive values, but not enough to reverse their sign. ΔG values are also positive and amount to between 22 and 25 kcal/mol.

Considering naked cations is thus not favorable for the substitution, but such a situation is anyway rather improbable in biological media.

III.3.b. Hydrated Cations. To better describe the state of the cations within a physiological environment, we have considered hydrated cations, and several states of hydration: $[Ca(H_2O)_n]^{2+}$ with $n = 6$ or 7, coupled to $[Pb(H_2O)_m]^{2+}$ with $m = 5$, 6, or 7. These coordination numbers have been chosen according to experimental and theoretical results. The sole available experimental value reported for the hydration number of Pb^{2+} in aqueous solution comes from NMR data and provides $m = 5.7 \pm 0.2$,[33] and Car−Parrinello dynamic simulations have provided a mean value of m equal to 7.0, which has been reduced to 6.4 by considering a longer simulation.[34] This value corresponds to the time average of competitive and exchanging 5-, 6-, and 7-fold coordinations. The coordination number of hydrated Ca^{2+}

TABLE 4: Substitution ΔE and ΔG Values (kcal/mol) for Hydrated Cations, Namely $[Ca(H_2O)_6]^{2+}$ and $[Pb(H_2O)_m]^{2+}$ (m = 5, 6, or 7)

ΔE	$[Pb(H_2O)_5]^{2+}$	$[Pb(H_2O)_6]^{2+}$	$[Pb(H_2O)_7]^{2+}$
H_{opt} (1UOV_ Ca_1/Pb_1)	126	146	169
M_{opt} (1UOV_ Ca_1/Pb_1)	19	39	63
L_{opt} (1UOV_ Ca_1/Pb_1)	−18	2	25
T_{opt} (1UOV_ Ca_1/Pb_1)	−18	2	26
H_{opt}(1UOV_ Ca_2/Pb_2)	119	139	162
M_{opt} (1UOV_ Ca_2/Pb_2)	12	33	56
L_{opt} (1UOV_ Ca_2/Pb_2)	−19	2	25
T_{opt} (1UOV_ Ca_2/Pb_2)	−25	−4	19
H_{opt} (1UOV_ Ca_3/Pb_3)	136	156	180
M_{opt} (1UOV_ Ca_3/Pb_3)	29	50	73
L_{opt} (1UOV_ Ca_3/Pb_3)	−17	3	26
T_{opt} (1UOV_ Ca_3/Pb_3)	−22	−2	22
ΔG	$[Pb(H_2O)_5]^{2+}$	$[Pb(H_2O)_6]^{2+}$	$[Pb(H_2O)_7]^{2+}$
T_{opt} (1UOV_ Ca_1/Pb_1)	−8	7	14
T_{opt} (1UOV_ Ca_2/Pb_2)	−15	−1	6
T_{opt} (1UOV_ Ca_3/Pb_3)	−13	1	8

TABLE 5: Substitution ΔE and ΔG Values (kcal/mol) for Hydrated Cations, Namely $[Ca(H_2O)_7]^{2+}$ and $[Pb(H_2O)_m]^{2+}$ (m = 5, 6, or 7)

ΔE	$[Pb(H_2O)_5]^{2+}$	$[Pb(H_2O)_6]^{2+}$	$[Pb(H_2O)_7]^{2+}$
H_{opt}(1UOV_ Ca_1/Pb_1)	104	124	147
M_{opt} (1UOV_ Ca_1/Pb_1)	−3	17	41
L_{opt} (1UOV_ Ca_1/Pb_1)	−40	−20	3
T_{opt} (1UOV_ Ca_1/Pb_1)	−40	−20	3
H_{opt}(1UOV_ Ca_2/Pb_2)	96	117	140
M_{opt} (1UOV_ Ca_2/Pb_2)	−10	10	34
L_{opt} (1UOV_ Ca_2/Pb_2)	−41	−20	3
T_{opt} (1UOV_ Ca_2/Pb_2)	−47	−27	−3
H_{opt} (1UOV_ Ca_3/Pb_3)	114	134	158
M_{opt}(1UOV_ Ca_3/Pb_3)	7	27	51
L_{opt} (1UOV_ Ca_3/Pb_3)	−39	−19	4
T_{opt} (1UOV_ Ca_3/Pb_3)	−44	−24	0
ΔG	$[Pb(H_2O)_5]^{2+}$	$[Pb(H_2O)_6]^{2+}$	$[Pb(H_2O)_7]^{2+}$
T_{opt} (1UOV_ Ca_1/Pb_1)	−18	−3	2
T_{opt} (1UOV_ Ca_2/Pb_2)	−26	−11	−6
T_{opt} (1UOV_ Ca_3/Pb_3)	−23	−9	−4

varies between 7 and 8,[35−37] depending on the simulations performed [see ref 38 and discussion therein].

Let us first consider $[Ca(H_2O)_6]^{2+}$, and, consequently, the following substitution reactions with m = 5, 6, or 7:

$$[Pb(H_2O)_m]^{2+} + (6-m)\cdot H_2O + [1UOV\_Ca_n] \rightarrow [1UOV\_Pb_n] + [Ca(H_2O)_6]^{2+}$$

As revealed by Table 4, for m = 7, all energy values are positive, whatever the site and whatever the level of optimization considered: no substitution is expected to occur. For m = 6, the situation is still not encouraging. The most interesting situation occurs for m = 5. For the three sites, the values of ΔE become negative, and thus favorable, from the L_{opt} optimization level. The ΔG values are also negative, which makes the substitution reactions favorable for the three model sites of synaptotagmin.

We can now consider $[Ca(H_2O)_7]^{2+}$, and the following substitution reactions, still with m = 5, 6, or 7:

$$[Pb(H_2O)_m]^{2+} + (7-m)\cdot H_2O + [1UOV\_Ca_n] \rightarrow [1UOV\_Pb_n] + [Ca(H_2O)7]^{2+}$$

As shown in Table 5, we now face many cases exhibiting negative reaction energies. For m = 7, ΔE values are positive, but entropy leads to negative ΔG values, except for the 1UOV_Pb_1 site. For m = 6, the ΔG values are negative, and more favorable than when $[Ca(H_2O)_6]^{2+}$ is considered. These values are still more favorable for m = 5. In fact, for m = 6, the ΔE values become negative as soon as the L_{opt} optimization level is considered (and even from the M_{opt} level for the 1UOV_ Ca_1/Pb_1 and 1UOV_ Ca_2/Pb_2 substitutions).

We can thus conclude that the substitution reactions are favorable for the three model sites of synaptotagmin for the two following reactions:

$$[Pb(H_2O)_5]^{2+} + 2H_2O + [1UOV\_Ca_n] \rightarrow [1UOV\_Pb_n] + [Ca(H_2O)_7]^{2+}$$

$$[Pb(H_2O)_6]^{2+} + H_2O + [1UOV\_Ca_n] \rightarrow [1UOV\_Pb_n] + [Ca(H_2O)_7]^{2+}$$

Moreover, the following reaction is also favorable:

$$[Pb(H_2O)_5]^{2+} + H_2O + [1UOV\_Ca_1] \rightarrow [1UOV\_Pb_1] + [Ca(H_2O)_6]^{2+}$$

The rather large substitution ΔG values obtained for these cases show that cationic exchange can occur, with no hope for reversibility. Once Pb^{2+} has replaced Ca^{2+} in a given site, not only has this site lost its capability to deal with Ca^{2+} cations but also, in view of the structural disorders induced, even the two other Ca^{2+} sites might be perturbed and, maybe, unable to host other Ca^{2+} cations. This could be especially true for sites 1 and 2, the calcium cations of which are only 3.71 Å far apart from one another.

IV. Conclusions

In the present contribution, the quantum chemistry protocols previously applied to investigate Ca^{2+} and Zn^{2+} substitutions by Pb^{2+} in the calmodulin and ALAD enzymes has been applied to model sites of synaptotagmin, an enzyme experimentally known to be targeted by lead.

It appears that such a cation exchange is thermodynamically allowed in any of the three Ca^{2+}-coordinating sites of synaptotagmin. Beyond favorable energetical values, such an exchange implies drastic structural reorganizations: even localized at a given site, such perturbations may preclude the enzyme to have any efficient role.

Acknowledgment. The computations have been performed on the national IDRIS (F. 91403 Orsay, France), CRIHAN (F. 76800 Saint-Etienne-du-Rouvray, France), and CINES (F. 34097 Montpellier, France) supercomputing centers. Some ELF computations have been run at the local CCRE centre at Université Pierre et Marie Curie, Univ Paris 6 (F. 75252 Paris CEDEX 05, France). Support from the French National Research Agency (ANR) on project SATURNIX (no. 2008-CESA-020) is acknowledged.

References and Notes

(1) Matthew, W. D.; Tsavaler, L.; Reichardt, L. F. *J. Cell Biol.* **1981**, *91*, 257.

(2) Perin, M. S.; Brose, N.; Jahn, R.; Sudhof, T. C. *J. Biol. Chem.* **1991**, *266*, 623.

(3) Perin, M. S.; Fried, V. A.; Mignery, G. A.; Jahn, R.; Sudhof, T. C. *Nature* **1990**, *345*, 260.

(4) Garcia, R. A.; Godwin, H. A. *Biophys. J.* **2004**, *86*, 2455.

(5) Suszkiw, J. B. *NeuroToxicology* **2004**, *25*, 599.

(6) Gourlaouen, C.; Parisel, O. *Int. J. Quantum Chem.* **2008**, *108*, 1888.

(7) Gourlaouen, C.; Parisel, O. *Angew. Chem. Intl. Ed.* **2007**, *46*, 553; *Angew. Chem.* **2007**, *119*, 559.

(8) Berman, H. M.; Westbrook, J.; Feng, Z.; Gilliland, G.; Bhat, T. N.; Weissig, H.; Shindyalov, I. N.; Bourne, P. E. *Nucleic Acids Res.* **2000**, *28*, 235.

(9) Frisch, M. J.; Trucks, G. W.; Schlegel, H. B.; Scuseria, G. E.; Robb, M. A.; Cheeseman, J. R.; Montgomery, J. A., Jr.; Vreven, T.; Kudin, K. N.; Burant, J. C.; Millam, J. M.; Iyengar, S. S.; Tomasi, J.; Barone, V.; Mennucci, B.; Cossi, M.; Scalmani, G.; Rega, N.; Petersson, G. A.; Nakatsuji, H.; Hada, M.; Ehara, M. Toyota, K.; Fukuda, R.; Hasegawa, J.; Ishida, M.; Nakajima, T.; Honda, Y.; Kitao, O.; Nakai, H.; Klene, M.; Li, X.; Knox, J. E.; Hratchian, H. P.; Cross, J. B.; Bakken, V.; Adamo, C.; Jaramillo, J.; Gomperts, R.; Stratmann, R. E.; Yazyev, O.; Austin, A. J.; Cammi, R.; Pomelli, C.; Ochterski, J. W.; Ayala, P. Y.; Morokuma, K.; Voth, G. A.; Salvador, P.; Dannenberg, J. J.; Zakrzewski, V. G.; Dapprich, S.; Daniels, A. D.; Strain, M. C.; Farkas, O.; Malick, D. K.; Rabuck, A. D.; Raghavachari, K.; Foresman, J. B.; Ortiz, J. V.; Cui, Q.; Baboul, A. G.; Clifford, S.; Cioslowski, J.; Stefanov, B. B.; Liu, G.; Liashenko, A.; Piskorz, P.; Komaromi, I.; Martin, R. L.; Fox, D. J.; Keith, T.; Al-Laham, M. A.; Peng, C. Y.; Nanayakkara, A.; Challacombe, M.; Gill, P. M. W.; Johnson, B.; Chen, W.; Wong, M. W.; Gonzalez, C.; Pople, J. A. *Gaussian 03*, Revision C.02; Gaussian, Inc.: Wallingford, CT, 2004.

(10) Lee, C.; Yang, W.; Par, R. G. *Phys. Rev. B* **1988**, *37*, 785.

(11) Becke, A. D. *J. Chem. Phys.* **1993**, *98*, 5648.

(12) Benjelloun, A. T.; Daoudi, A.; Chermette, H. *J. Chem. Phys.* **2004**, *121*, 7207.

(13) Benjelloun, A. T.; Daoudi, A.; Chermette, H. *Mol. Phys.* **2005**, *103*, 317.

(14) Benjelloun, A. T.; Daoudi, A.; Chermette, H. *J. Chem. Phys.* **2005**, *122*, 154304.

(15) Gourlaouen, C.; Piquemal, J.-P.; Saue, T.; Parisel, O. *J. Comput. Chem.* **2006**, *27*, 142.

(16) Gourlaouen, C.; Piquemal, J.-P.; Parisel, O. *J. Chem. Phys.* **2006**, *124*, 174311.

(17) For a recent review, see, for example: Dolg, M. In *Modern Methods and Algorithms of Quantum Chemistry*; Grotendorst, J., Ed.; John von Neumann Institute for Computing: Jülich, 2000. Stoll, H.; Metz, B.; Dolg, M. *J. Comput. Chem.* **2002**, *23*, 767.

(18) Kuelche, W.; Dolg, M.; Stoll, H.; Preuss, H. *Mol. Phys.* **1991**, *74*, 1245.

(19) Gourlaouen, C.; Piquemal, J.-P.; Parisel, O. *Chem. Phys. Lett.* **2009**, *469*, 38.

(20) van Severen, M.-C.; Gourlaouen, C.; Parisel, O. *J. Comput. Chem.* **2010**, *31*, 185.

(21) Gourlaouen, C.; Gérard, H.; Piquemal, J.-P.; Parisel, O. *Chem.—Eur. J.* **2008**, *14*, 2730.

(22) Noury, S.; Krokidis, X.; Fuster, F.; Silvi, B. TopMod Package, 1997. *This package is available on the web site of the Laboratoire de Chimie Théorique*; Université Pierreet Marie Curie (UMR 7616, CNRS: Paris 6 -UPMC, URL: www.lct.jussieu.fr (see the personal home page of Prof. B. Silvi).

(23) Noury, S.; Krokidis, X.; Fuster, F.; Silvi, B. *Comput. Chem. (Oxford)* **1999**, *23*, 597.

(24) Becke, A. D.; Edgecombe, K. E. *J. Chem. Phys.* **1990**, *92*, 5397.

(25) Savin, A.; Nesper, R.; Wengert, S.; Fässler, T. F. *Angew. Chem. Intl. Ed.* **1997**, *36*, 1808; *Angew. Chem.* **1997**, *109*, 1892.

(26) Silvi, B.; Savin, A. *Nature* **1994**, *371*, 683.

(27) Savin, A.; Silvi, B.; Colonna, F. *Can. J. Chem.* **1996**, *74*, 1088.

(28) Piquemal, J.-P.; Pilmé, J.; Parisel, O.; Gérard, H.; Fourré, I.; Bergès, J.; Gourlaouen, C.; de la Lande, A.; van Severen, M.-C.; Silvi, B. *Int. J. Quantum Chem.* **2008**, *108*, 1951.

(29) Kohout, M.; Savin, A. *J. Comput. Chem.* **1997**, *18*, 2000.

(30) Joubert, L.; Silvi, B.; Picard, G. *Theor. Chem. Acc.* **2000**, *104*, 109.

(31) Shimony-Livny, I.; Glusker, J. P.; Bock, C. W. *Inorg. Chem.* **1988**, *37*, 1853.

(32) van Severen, M.-C.; Piquemal, J.-P.; Parisel, O. *Chem. Phys. Lett.* **2009**, *478*, 17.

(33) Swift, T. J.; Sayre, W. G. *J. Chem. Phys.* **1966**, *44*, 3567.

(34) Gourlaouen, C.; Gérard, H.; Parisel, O. *Chem.—Eur. J.* **2006**, *12*, 5024.

(35) Lightstone, F. C.; Schwegler, E.; Hood, R. Q.; Gygi, F.; Galli, G. *Chem. Phys. Lett.* **2001**, *343*, 549.

(36) Badyal, Y. S.; Barnes, A. C.; Cuello, G. J.; Simonson, J. M. *J. Phys. Chem. A* **2004**, *108*, 11819.

(37) Jalilehvand, F.; Spangberg, D.; Linvquist-Reis, P.; Hermansson, K.; Persson, I.; Sandström, M. *J. Am. Chem. Soc.* **2001**, *123*, 431.

(38) Piquemal, J.-P.; Perera, L.; Cisneros, G. A.; Ren, P.; Pedersen, L. G.; Darden, T. A. *J. Chem. Phys.* **2006**, *125*, 054511.

JP910131R